

Low-Frequency Chain Dynamics of Poly(*n*-hexyl methacrylate) by Dielectric Spectroscopies

E. Dudognon,* A. Bernès, and C. Lacabanne

Laboratoire de Physique des Polymères, Université Paul Sabatier, 31062 Toulouse Cedex 04, France

Received December 27, 2001

ABSTRACT: The study of poly(*n*-hexyl methacrylate) has been performed by both thermo-stimulated currents (TSC) and dynamic dielectric spectroscopy (DDS) in order to better define the nature of molecular mobility in the glass transition temperature range. TSC results reveal the existence of three dipolar relaxation modes: α , ascribed to the glass relaxation; β , assigned to a secondary relaxation mode; and α' , associated with the dielectric manifestation of the liquid–liquid transition. DDS allowed us to follow the merging of the α and β modes as frequency increases from 10^{-2} to 10^6 Hz. Then the fractional polarizations protocol permitted us to define at low frequency (10^{-3} – 10^{-2} Hz) the fine structure of these complex relaxations: relaxation times isolated for the β and α modes are widely distributed and obey an Arrhenius law while those isolated for the α' mode are narrowly distributed and are better defined by a Vogel–Tamman–Fulcher law. Finally, the evolution of the activation enthalpy helps us to precise the nature of involved molecular movements.

Introduction

Although a lot of research has been performed on the glass transition of polymers, the nature of molecular mobility in this temperature range is still unclear. The thermo-stimulated currents technique (TSC)¹ appears as a powerful tool to study this temperature range on account of its low equivalent frequency ($\sim 10^{-3}$ Hz). Previously published results obtained on an amorphous polymer, the poly(*n*-butyl methacrylate) (PnBMA),² show that the high resolution of this technique allowed us to reveal the existence around the glass transition of two dipolar relaxations: the glass relaxation and, at higher temperature, another one that we assigned to the dielectric manifestation of the liquid–liquid transition. We also reported an evolution of the behavior law of relaxation times and a hierarchy of molecular movements.

On the other hand, dynamic dielectric spectroscopy (DDS) allows us to follow the evolution of complex relaxations on a large frequency scale (10^{-2} – 10^6 Hz).

We have thus realized the study, in the glass transition temperature range, of an amorphous model polymer, by both TSC and DDS. First, the TSC technique allowed us to determine, at low frequencies (10^{-3} – 10^{-2} Hz), the relaxation modes around the glass transition, and the fractional polarizations protocol permitted us to describe the fine structure of these complex relaxations by structural parameters (activation enthalpy ΔH and activation entropy ΔS). Then, DDS experiments allowed us to follow the evolution of these relaxations on a large frequency scale (10^{-2} – 10^6 Hz). The comparison of obtained results will help us to improve the understanding of low-frequency chain dynamics.

The chosen model polymer is the poly(*n*-hexyl methacrylate) (PnHMA). Since it belongs to the same series as PnBMA but with a longer alkyl side group, results could be compared with our previous findings. Moreover, this material has been the subject of recent studies by Beiner et al. by dynamic shear modulus³ between 10^{-1}

and 10^1 Hz and by heat capacity spectroscopy (HCS)^{4,5} between 10^{-1} and 10^3 Hz. By the latter technique, it exhibited a particular behavior in this frequency range that we could link to our DDS results.

Experimental Section

1. Materials. PnHMA used in this study was furnished by PolymerExpert. It was synthesized by anionic polymerization in order to control the tacticity (85% syndiotactic). The molecular weight was chosen high enough to provide samples with good thermomechanical stability: $M_n = 93\,000$ g mol⁻¹ estimated by size exclusion chromatography with polystyrene standard. The polydispersity index is 2.22. Samples were then prepared in the form of films. The glass transition temperature was estimated by differential scanning calorimetry. Experiments were carried out at 10 °C/min, and the glass transition was determined by the inflection point method. We found T_g close to -5 °C.

2. Methods. (i) TSC Spectra. Complex Spectra. In the TSC technique,¹ the sample is polarized by an electrical field E at a temperature T_p for a time t_p ($t_p = 2$ min), which allows all dipolar units having relaxation time $\tau(T_p)$ lower than t_p to orient. The sample is then quenched to a temperature $T_0 \ll T_p$ with liquid nitrogen, which freezes the orientation of dipoles. At this temperature, the electrical field is cut off and the sample is short-circuited for t_0 ($t_0 = 2$ min) in order to eliminate surface charges. Upon heating at 7 °C min⁻¹, dipolar units return to equilibrium, and a depolarization current is recorded with a Keithley 642 electrometer with a precision of 10^{-16} A.

Elementary Spectra. The recorded global spectrum is generally complex because it results from the distribution of species with different relaxation times. To resolve this wide distribution of relaxation times, different approaches exist: an analytical one with the use of function fits with continuous parameters (for example, a Kohlrausch–Williams–Watts function⁶) and an experimental one, namely, the fractional polarization protocol, which permits to resolve experimentally the fine structure of the complex spectra.¹ For this work, we chose the last one. In this procedure, after polarization at T_p for t_p ($t_p = 2$ min), the sample is short-circuited for t_d ($t_d = 2$ min) at T_d some degrees below the polarization temperature. Thus, dipolar units characterized by relaxation times τ such that $\tau(T_p)$ is lower than t_p and $\tau(T_d)$ is higher than t_d are oriented and experimentally isolated. The sample is then quenched, and as for the TSC experiment, the depolarization

* Corresponding author: Tel 33 5 61 55 65 39; Fax 33 5 61 55 62 21; e-mail e_dudognon@yahoo.fr.

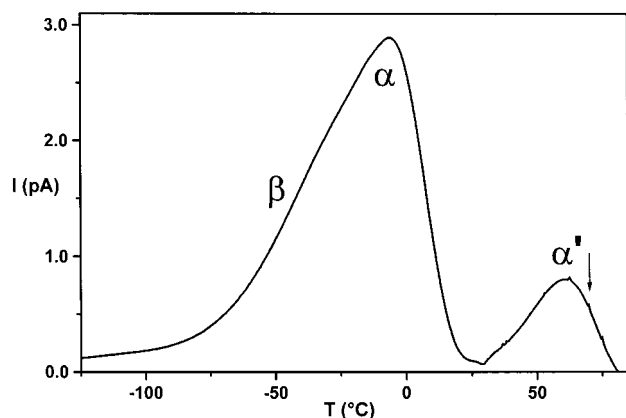


Figure 1. Complex TSC spectrum of PnHMA polarized at 70 °C (indicated by the arrow) by an applied electrical field of $9.6 \times 10^5 \text{ V m}^{-1}$.

current is recorded upon a linear increase of temperature. By shifting the polarization window ($\Delta T = T_p - T_d$) along the temperature axis, a series of elementary spectra are obtained.

In such a heterogeneous approach, a Debye type process characterized by a single relaxation time $\tau(T)$ is associated with each elementary spectrum. These $\tau(T)$ can be calculated from the recorded depolarization current $I(T)$:

$$\tau(T) = \frac{1}{qI(T)} \int_T^\infty I(T) dT$$

where $q = dT/dt$ is the heating rate.

(ii) DDS Spectra. A broadband dielectric spectrometer Novocontrol BDS 4000 was used to measure the complex dielectric function $\epsilon^*(\omega)$, in the temperature range from -60 to 60 °C and in the frequency range from $\omega = 2\pi \times 10^{-2}$ to $\omega = 2\pi \times 10^6 \text{ rad s}^{-1}$.

To extract the Havriliak–Negami relaxation times τ_{HN} , a mean relaxation time that takes into account the width and the asymmetry of the mode, the results were fitted by a sum of one or two Havriliak–Negami functions:⁷

$$\epsilon^*(\omega) = \epsilon'(\omega) - i\epsilon''(\omega) = \epsilon_\infty + \frac{\Delta\epsilon}{[1 + (i\omega\tau_{\text{HN}})^{\alpha_{\text{HN}}}]^{\beta_{\text{HN}}}}$$

where $\epsilon'(\omega)$ and $\epsilon''(\omega)$ are respectively the real and the imaginary parts of the complex permittivity, ϵ_∞ is the real permittivity for high frequencies, $\Delta\epsilon$ is the relaxation strength, and α_{HN} and β_{HN} are the Havriliak–Negami parameters.

Results

TSC Complex Spectrum. The complex TSC spectrum of PnHMA is reported in Figure 1: a sample of 125 μm was polarized at 70 °C by an applied electrical field of $9.6 \times 10^5 \text{ V m}^{-1}$. Two peaks can be observed: the first one, labeled α , appears at -5 °C; the second one, α' , is located at 60 °C. The effect on this spectrum of the variation of the polarization temperature can be seen in Figure 2 where T_p varies between -50 and 70 °C. In this figure, the existence of another peak, β , appearing approximately at -30 °C is established. It is progressively hidden by the α peak when T_p is increased and appears then as a shoulder of this peak.

To define the origin of these modes, we checked their reproducibility, and we verified that they were not due to conduction effects, surface charges, or ions resulting from the polymerization. We also checked that PTFE blocking electrodes do not modify the TSC α' peak. Finally, the linear variation of the polarization of each peak with the applied electrical field allowed us to

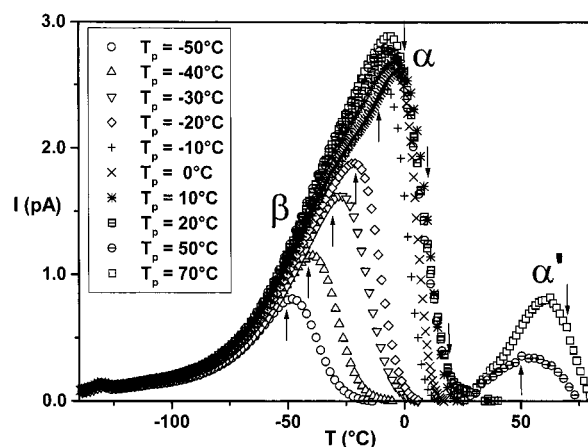


Figure 2. Influence of polarization temperature on TSC complex spectrum of PnHMA. The applied electrical field is $9.6 \times 10^5 \text{ V m}^{-1}$. The polarization temperature is varying from -50 to 70 °C as indicated by the arrows.

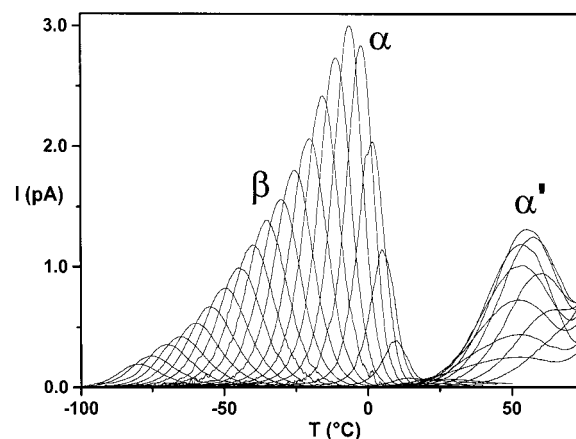


Figure 3. Fine structure of PnHMA obtained by fractional polarizations method. The applied electrical field is $2.8 \times 10^6 \text{ V m}^{-1}$, and the polarization window of 5 deg is shifted along the temperature axis by 5 deg between -90 and 80 °C.

establish that all these relaxation modes are dipolar and not due to the interfacial polarization process.

Moreover, since the maximum temperature of the α peak agrees with the glass transition temperature determined by the differential scanning calorimetry experiment, we ascribed this mode with the dielectric manifestation of the glass transition. The β mode is a secondary relaxation mode assigned in the bibliography to the motion of the alkyl group⁸ and, more precisely, to π flip motion of this group around the C–C bond that links it to the main chain, coupled to a small rotation of the chain backbone around its local chain axis, as reported by Schmidt-Rohr and co-workers on PMMA,⁹ PEMA,¹⁰ or PnBMA.¹¹

As for the α' mode, we ascribed this relaxation, in agreement with previous work on PnBMA,² to the dielectric manifestation of the liquid–liquid transition.¹²

Fine Structure of TSC Spectra. The fine structure of this complex spectrum was obtained by the fractional polarizations protocol. The sample (85 μm thickness) was polarized by an applied electrical field of $2.8 \times 10^6 \text{ V m}^{-1}$. The polarization window of 5 deg was shifted by 5 deg between -90 and 80 °C. The series of obtained elementary spectra is reported in Figure 3.

In this figure, we remark that the envelope of the series follows the shape of the complex spectrum. We also note a clear behavior difference between, on one

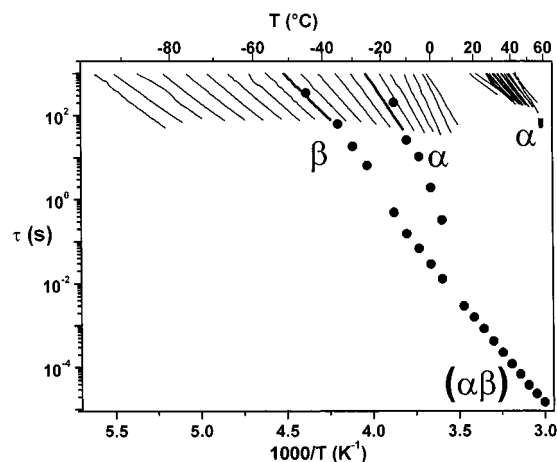


Figure 4. Comparison on an Arrhenius diagram of relaxation times extracted on one hand by fractional polarizations (—) (elementary relaxation times) and on the other hand by DDS (●) (mean relaxation times).

hand, the β and the α modes and, on the other hand, the α' mode. Indeed, the elementary spectra isolated for the β and the α modes are progressively shifted toward higher temperatures with the polarization window, which indicates a wide distribution of relaxation times. On the contrary, the elementary spectra isolated until the α' mode maximum are almost independent of the polarization conditions since the temperature of the peaks maximum is constant. This reveals a narrow distribution of relaxation times. Such a behavior difference has already been reported in the case of PnBMA.² It should be noted that, from the mode maximum, peaks are shifted to higher temperatures because of the appearance of conductivity.

Assuming a single relaxation time, we can calculate for each elementary peak, by using the Debye's model, the variation of the associated relaxation time τ . The variations of these τ are reported in the upper part of an Arrhenius diagram in Figure 4 (lines between 10^{-2} and 10^{-3} Hz). The variations of relaxation times associated with elementary spectra isolated for the β and the α modes are linear in this diagram, and they obey an Arrhenius equation:

$$\tau(T) = \tau_{0a} \exp\left[\frac{\Delta H}{RT}\right]$$

where τ_{0a} is a preexponential factor that can be related to the activation entropy, ΔH is the activation enthalpy, and R is the perfect gas constant.

This behavior is typical of secondary and glass relaxations studied by the fractional polarization protocol and analyzed in a heterogeneous approach.¹

As for the elementary spectra isolated for the α' mode, variations of τ are not linear in the Arrhenius diagram, and they are better fitted by a Vogel–Tamman–Fulcher law:

$$\tau(T) = \tau_{0v} \exp\left[\frac{1}{\alpha_f(T - T_\infty)}\right]$$

where τ_{0v} is a preexponential factor, α_f is the thermal expansion coefficient of the free volume, and T_∞ is the critical temperature at which any mobility is frozen.

Such a behavior has already been observed in the case of PnBMA,² contrary to the PMMA or PEMA, which will be the subject of forthcoming publication.

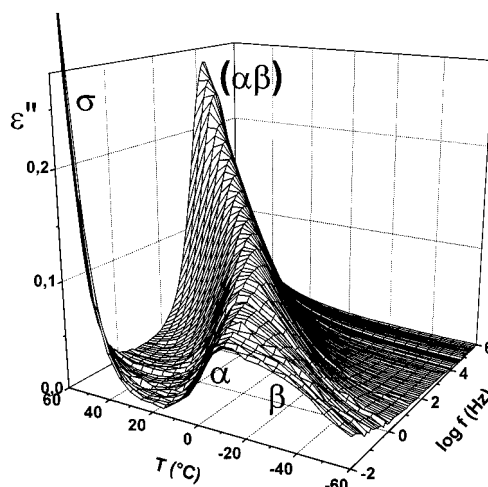


Figure 5. Evolution of ϵ'' between -60 and 60 °C and 10^{-2} and 10^6 Hz for PnHMA.

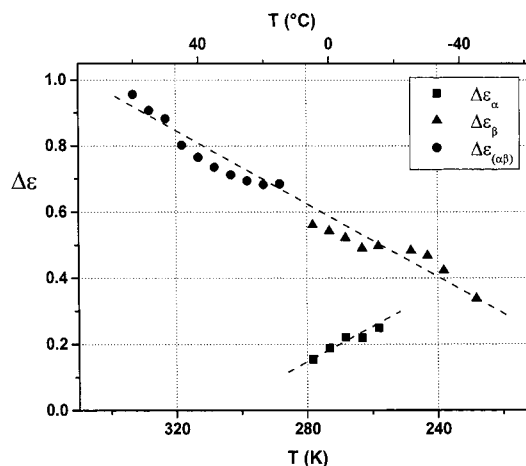


Figure 6. Evolution with temperature of the relaxation strength, $\Delta\epsilon$, of the α , β , and $(\alpha\beta)$ modes. Dashed lines are guides for the eye.

We found for the most intense elementary spectrum $T_\infty = -61 \pm 2$ °C, $\tau_{0v} = (2 \pm 7) \times 10^{-3}$ s, and $\alpha_f = 8.2 \times 10^{-3} \pm 9 \times 10^{-4}$ K⁻¹.

DDS Relaxation Map. The recording of the variation of ϵ'' between 10^{-2} and 10^6 Hz and -60 °C and 60 °C by dynamic dielectric spectroscopy measurement is reported in Figure 5.

In this three-dimensional representation, we make out the β and the α relaxation modes that merge when frequency increases and lead to a new mode, called $(\alpha\beta)$ or a in the bibliography. This merging phenomenon is indeed observed in the series of poly(*n*-alkyl methacrylates).¹³ Furthermore, we have reported in Figure 6 the relaxation strength variations, $\Delta\epsilon$, of the α , β , and $(\alpha\beta)$ modes. As can be seen, as frequency increases and the α mode converges to the β mode, its amplitude decreases, and it disappears before it reaches the β mode. Meanwhile, the amplitude of the β mode keeps on increasing until it reaches the $(\alpha\beta)$ mode. These results are in agreement with those previously established for PEMA and PnBMA by Garwe and co-workers¹³ and especially for PnHMA by Beiner and co-workers.^{4,5} Indeed, they reported the same evolution of $\Delta\epsilon$ for DDS experiments (although amplitudes we found are a bit lower), and their study by HCS revealed a saddle between the α and $(\alpha\beta)$ modes. It should be noted that we did not increase the temperature high enough to

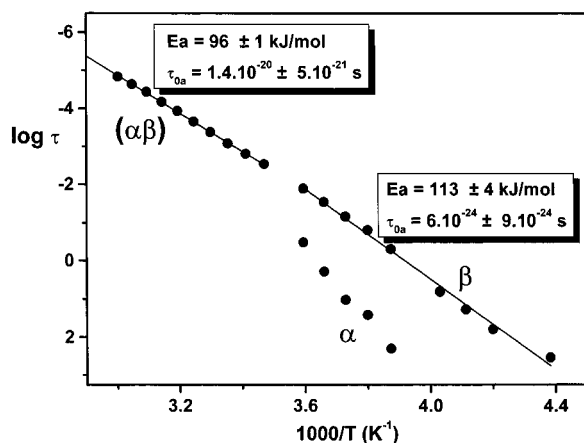


Figure 7. Arrhenius diagram of Havriliak–Negami relaxation times associated with α , β , and $(\alpha\beta)$ modes (●). The lines represent Arrhenius fits.

observe a decrease of the $(\alpha\beta)$ intensity at high temperature.

At high temperature and low frequency, a conductivity phenomenon is also observed in Figure 5.

By using the Havriliak–Negami model, the Havriliak–Negami relaxation time τ_{HN} associated with each complex relaxation mode can be extracted. Their variations are reported in an Arrhenius diagram in Figure 7. As can be seen, τ_{HN} associated with the β and $(\alpha\beta)$ modes are well fitted by an Arrhenius law, which is in agreement with previous results found by Garwe et al. on other poly(*n*-alkyl methacrylates), especially PEMA and PnBMA¹³ (b zone for the $(\alpha\beta)$ mode and c zone for the β mode). We found an activation energy of 96 ± 1 and 113 ± 4 kJ mol⁻¹ respectively for the $(\alpha\beta)$ and the β modes. These fitting parameters are of the same order as those reported for the first samples of the series although they are either a bit lower for the $(\alpha\beta)$ process or a bit higher for the β process, which is due to the influence of the alkyl side group length. As for the preexponential factors, they are lower than the value expected for a localized motion (10^{-13} s), which suggests cooperative motions on a very small scale. As far as the α mode is concerned, the relaxation time seems better described by a Vogel–Tamman–Fulcher law, as generally observed for the glass relaxation by dynamic dielectric or mechanical⁸ experiments, even if we could not define significant fitting parameters due to the lack of experimental data.

Discussion

Comparison of TSC and DDS results allows us to compare results concerning complex relaxations on a large frequency scale (10^{-2} – 10^6 Hz) with results concerning the fine structure of these relaxations at lower frequencies (10^{-3} – 10^{-2} Hz).

Evolution of Relaxations between 10^{-3} and 10^6 Hz. In Figure 4, mean relaxation times extracted with Havriliak–Negami's model from DDS spectra (lower part) and elementary relaxation times calculated with Debye's model from the elementary spectra isolated by the fractional polarizations method (upper part) are reported in the same Arrhenius diagram.

From the comparison of results obtained by both techniques, we saw that, as the β mode is concerned, the τ_{HN} obtained by DDS and associated with the complex relaxation corresponds to an elementary relaxation time isolated by the fractional polarizations

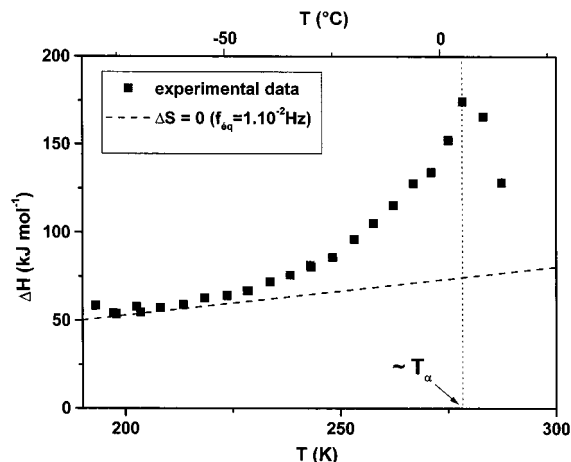


Figure 8. Evolution of activation enthalpy as a function of peak maximum temperature (accuracy of 5%). The dashed line is Starkweather's "line" of $\Delta S = 0$ (calculated with an equivalent frequency of 10^{-2} Hz).

method close to the maximum of the β mode (in the temperature range of the shoulder, due to the β mode, observed in the complex TSC spectrum). This emphasizes the agreement in temperature between our results. Moreover, in both cases, relaxation times obey an Arrhenius equation, which confirms the localized nature of involved motions.

As the α mode is concerned, we also note a good agreement in temperature between the τ_{HN} extracted from DDS results and the TSC relaxation time that is associated with the elementary spectrum isolated at the mode maximum. However, we found by both techniques different behavior laws: the τ extracted from TSC results (10^{-3} – 10^{-2} Hz) obeys an Arrhenius equation whereas the τ_{HN} (10^{-2} – 10^6 Hz) seems better described by a Vogel–Tamman–Fulcher law. This crossover has previously been reported by Colmenero¹⁴ and Menegotto.¹⁵ This phenomenon is assigned to the change of thermodynamic state of the sample at the glass transition: in DDS experiments, sample is in an equilibrium thermodynamic state whereas it is in a vitreous metastable state in TSC experiments.

As for the α' mode, the appearance of conductivity by DDS prevented us from observing a relaxation mode in this temperature and frequency range.

Activation Enthalpy Evolution at Low Frequencies. From fractional polarizations results, we can determine structural parameters as ΔH and ΔS . We then studied the activation enthalpy evolution toward the β and the α modes.

In Figure 8, the variation of activation enthalpies of elementary processes isolated in the β and α modes temperature range is reported as a function of peak maximum temperature. We added Starkweather's "line"¹⁶ corresponding to the theoretical activation enthalpy ΔH_0 (for a null activation entropy). It can be written as

$$\Delta H_0 = RT \left[1 + \ln \left(\frac{kT}{2\pi h f_{\text{eq}}} \right) \right]$$

where h is Planck's constant and f_{eq} is the equivalent frequency ($\approx 1 \times 10^{-2}$ Hz).

In that figure, we observe that the activation enthalpy in the temperature range of the β mode follows Starkweather's "line", which indicates, according to Stark-

weather's cooperativity criterion,¹⁷ that motions are localized and noncooperative ($\Delta S = 0$).

As the α mode is concerned, the behavior is quite different. Indeed, as observed in PnBMA,² it can be divided in two parts.

Until the mode maximum, the activation enthalpy increases and departs from the null activation entropy "line". This rough increase, first, permits us to distinguish clearly this mode from the β mode. Second, it indicates a simultaneous increase of activation entropy. The movement is more delocalized and more cooperative.

Above the α mode maximum, activation enthalpy and entropy decrease: the interactions between mobile units and their environment are getting lower.

It should be noted that the maximum activation enthalpy is lower than in PnBMA and in the first polymethacrylates of the series as will be published elsewhere. That reveals that cooperativity decreases. This conclusion can be compared with previous DDS results: it agrees with Donth's conclusion. Indeed, dynamic dielectric studies showed that, as the alkyl group increases, the merging zone of the α and β modes is progressively shifted to lower temperatures and frequencies.¹³ Thus, at fixed frequency, as in TSC studies, the longer the alkyl group, the nearer the merging zone is approached. According to Donth et al., as the merging point is approached, the cooperativity of the α mode decreases.¹⁸ This could explain the absence, contrary to the case of PMMA, PEMA,¹⁹ or PnBMA,² of a compensation phenomenon² that, generally, emphasizes the existence of cooperativity. The molecular mobility could be sufficiently cooperative to provoke the shift of the activation enthalpy from Starkweather's "line" but not enough cooperative to generate a compensation phenomenon, which would reinforce Dargent's conclusions on the compensation law.²⁰

Conclusion

This study of PnHMA by thermo-stimulated currents and dynamic dielectric spectroscopy emphasizes the complementarity between these two techniques.

On one hand, the use of the thermo-stimulated currents allowed us to show the existence at low frequencies (10^{-3} – 10^{-2} Hz) of three dipolar relaxation modes: a glass relaxation, α , at -5 °C, a secondary relaxation mode, β , at -30 °C associated with a π flip motion of the alkyl group around the bond that links it to the main chain, coupled to a small rotation of the chain backbone around its local chain axis, and an other relaxation mode, α' , at 60 °C which we assigned to the dielectric manifestation of the liquid–liquid transition.

On the other hand, dynamic dielectric spectroscopy experiments permitted us to follow the evolution of these complex relaxations on a large frequency scale (10^{-2} – 10^6 Hz). We observed the merging, when frequency increases, of the α and β modes as previously reported

for other poly(*n*-alkyl methacrylates): the α mode disappears before it reaches the β mode.

Furthermore, the use of the fractional polarizations protocol allowed us to determine, at low frequencies (10^{-3} – 10^{-2} Hz), the fine structure of these complex relaxations. A close similarity appears between these results and those previously found for PnBMA: at low frequencies, relaxation times associated with the β and α modes are largely distributed and obey an Arrhenius law while those associated with the α' mode are narrowly distributed and are better fitted by a Vogel–Tamman–Fulcher law. At higher frequencies, we note a crossover from an Arrhenius behavior to a Vogel–Tamman–Fulcher one for the α mode. Moreover, the evolution of structural parameters confirms the establishment of hierarchically correlated molecular mobility, found for PnBMA: as temperature increases across the glass transition, movements are more and more delocalized.

References and Notes

- (1) Teyssedre, G.; Mezghani, S.; Bernes, A.; Lacabanne, C. In *Dielectric Spectroscopy of Polymeric Materials: Fundamentals and Applications*; Runt, J. P., Fitzgerald, J. J., Eds.; American Chemical Society: Washington, DC, 1997; Chapter 8, pp 227–258.
- (2) Dudognon, E.; Bernès, A.; Lacabanne, C. *Macromolecules* **2001**, *34*, 3988–3992.
- (3) Beiner, M.; Schröter, K.; Hempel, E.; Reissig, S.; Donth, E. *Macromolecules* **1999**, *32*, 6278–6282.
- (4) Beiner, M.; Kahle, S.; Hempel, E.; Schröter, K.; Donth, E. *Europhys. Lett.* **1998**, *44*, 321–327.
- (5) Beiner, M.; Kahle, S.; Hempel, E.; Schröter, K.; Donth, E. *Macromolecules* **1998**, *31*, 8973–8980.
- (6) Alegria, A.; Goitiandia, L.; Colmenero, J. *J. Polym. Sci., Part B: Polym. Phys.* **2000**, *38*, 2105–2113.
- (7) Havriliak, S.; Negami, S. *J. Polym. Sci., Part C* **1966**, *14*, 99.
- (8) McCrum, N. G.; Read, B. E.; Williams, G. In *Anelastic and Dielectric Effects in Polymeric Solids*; J. Wiley: New York, 1991.
- (9) Schmidt-Rohr, K.; Kulik, A. S.; Beckham, H. W.; Ohlemacher, A.; Pawelzik, U.; Boeffel, C.; Spiess, H. W. *Macromolecules* **1994**, *27*, 4733–4745.
- (10) Kulik, A. S.; Beckham, H. W.; Schmidt-Rohr, K.; Radloff, D.; Pawelzik, U.; Boeffel, C.; Spiess, H. W. *Macromolecules* **1994**, *27*, 4746–4754.
- (11) Domberger, W.; Reichert, D.; Garwe, F.; Schneider, H.; Donth, E. *J. Phys.: Condens. Matter* **1995**, *7*, 7419–7426.
- (12) Boyer, R. F. *Encycl. Polym. Sci. Eng.* **1989**, *7*, 23–47.
- (13) Garwe, F.; Schönhals, A.; Lockwenz, H.; Beiner, M.; Schröter, K.; Donth, E. *Macromolecules* **1996**, *29*, 247–253.
- (14) Colmenero, J. *J. Non-Cryst. Solids* **1991**, *131–133*, 860–869.
- (15) Menegotto, J. Thesis, Paul Sabatier University, Toulouse, 1999.
- (16) Starkweather, H. W., Jr. *Macromolecules* **1981**, *14*, 1277–1281.
- (17) Starkweather, H. W., Jr. *Macromolecules* **1988**, *21*, 1798–1802.
- (18) Donth, E. *J. Polym. Sci., Part B: Polym. Phys.* **1996**, *34*, 2881–2892.
- (19) Sauer, B. B.; Avakian, P. *Polymer* **1992**, *33*, 5128–5142.
- (20) Dargent, E.; Kattan, M.; Cabot, C.; Lebaudy, P.; Ledru, J.; Grenet, J. *J. Appl. Polym. Sci.* **1999**, *74*, 2716–2723.

MA012243X